

Propagation of Target Waves in the Presence of Obstacles

J. A. Sepulchre and A. Babloyantz

Service de Chimie Physique, Université Libre de Bruxelles, CP 231, Boulevard du Triomphe, 1050 Brussel, Belgium

(Received 1 June 1990; revised manuscript received 10 January 1991)

The propagation of target waves in the presence of walls and windows is considered. It is shown that in a finite system, for sufficiently small passages no target waves are triggered. Propagation through a large opening can inhibit the onset of waves from smaller windows.

PACS numbers: 42.20.-y, 03.40.Kf

Concentric waves of chemical activity have been observed in reacting systems as well as in other media. The theoretical aspect of the problem has also drawn much attention from researchers in diverse fields.^{1,2} In this paper we report numerical simulations of target waves in a reaction-diffusion medium where a partition is introduced in the system. Two openings of various size insure the communication between the two compartments. In such an environment, target waves show some unexpected behavior which is the object of this Letter.

The reaction is assumed to proceed in a two-dimensional square vessel in the presence of diffusion. The compartment walls are subject to "no-flux" boundary conditions. The general equation describing this system is

$$\frac{\partial \mathbf{X}}{\partial t} = \mathbf{F}(\mathbf{X}) + D\nabla^2 \mathbf{X}, \quad (1)$$

where $\mathbf{X}(\mathbf{r}, t)$ is a vector representing the concentration variables and D is the diffusion matrix taken here to be a multiple of the identity matrix.

It is assumed that the reaction kinetics is such that for a range of parameter values a supercritical Hopf bifurcation leading to bulk oscillations takes place. Near the instability point, such a system may be reduced to a Ginzburg-Landau-type equation which characterizes the behavior of the slowly varying complex amplitude $A(\rho, \tau)$ defined as

$$\mathbf{X} - \mathbf{X}_0 = \xi \varepsilon^{1/2} A(\rho, \tau) e^{i\omega_0 t} + \text{c.c.}, \quad (2)$$

where \mathbf{X}_0 describes the concentration values of a steady solution of Eq. (1) which has become unstable via the Hopf bifurcation and ξ is the critical mode, i.e., the eigenvector related to the eigenvalue $i\omega_0$ of the Jacobian matrix of \mathbf{F} computed at \mathbf{X}_0 . The small parameter $\varepsilon \ll 1$ is a measure of the distance from the bifurcation point and the complex field $A(\rho, \tau)$ evolves on the slow time scale $\tau = \varepsilon t$ and on the large length scale $\rho = (\varepsilon/D)^{1/2} \mathbf{r}$. In the postcritical regime Eq. (1) gives³

$$\frac{\partial A}{\partial \tau} = \mu A - (g_r + ig_i) |A|^2 A + \nabla^2 A. \quad (3)$$

The real constants g_r , g_i , and μ can be related to the parameters of the model. In the case of a supercritical

bifurcation, we have μ and $g_r > 0$. With the help of the amplitude equation (3), one shows that to the lowest order in ε , the bulk frequency of the homogeneous oscillation of concentrations \mathbf{X} is $\Gamma = \omega_0 - \varepsilon \mu g_i / g_r$. When the nonlinear dispersion g_i is normal, i.e., when the period of the oscillations increases with the amplitude, then $g_i > 0$.

We first study the events in the compartment I when only one window is considered [Figs. 1(a) and 1(b)]. In the system described by Eq. (2), target waves may be generated around centers by introducing in the system local inhomogeneities that we shall call pacemaker centers. First, traveling waves are generated under the action of a small local fluctuation in the concentration variable. The waves generated by such a mechanism have a tendency to vanish after some time.⁴

Target waves also appear if the parameters of the pacemaker region are slightly different from the remaining part of the medium. In this paper the waves were

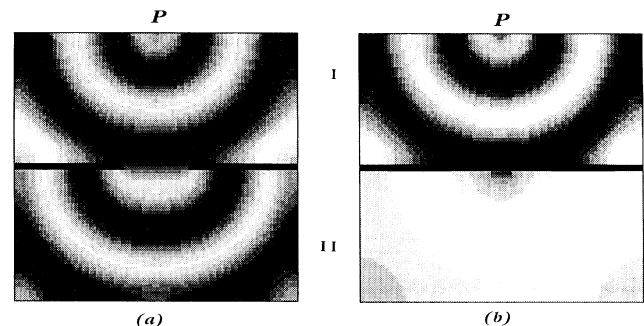


FIG. 1. (a),(b) A square vessel of side L is partitioned by a wall and communicates through a window of size l . A pacemaker region at P , where frequency is locally increased by $\Delta\omega$, generates target waves in compartment I, with a frequency Ω_1 . (a) The size of the window is $2l_c$ and in compartment II waves can propagate at the same frequency as in compartment I. (b) The size of the window is $\frac{2}{3}l_c$. No target waves are seen in compartment II for finite-size systems. The parameters of Eq. (4) are $\beta=1$, $\Delta\omega=1$. The critical window length is $l_c=5.03$ in units of the nondimensional space variable ρ' . The discretization of the vessel of side $L=44.8$ is 80×80 . The pacemaker at P is "T shaped," built on sixteen adjacent cells. The width of the wall is 1.12.

generated by a local frequency shift $\Delta\omega$ between the pacemaker region and the bulk. This center initiates target waves in the system which again propagate in concentric rings starting from the pacemaker center and gradually take over the entire vessel.

A practical way to describe the action of the pacemaker is to introduce a new term into Eq. (3):

$$\frac{\partial Z}{\partial \tau'} = [1 + i\Delta\omega(\rho')]Z - (1 + i\beta)|Z|^2Z + \nabla'^2 Z \quad (4)$$

and

$$A = (\mu/g_r)^{1/2}Z, \quad \beta = g_i/g_r, \quad \tau' = \mu\tau, \quad \rho' = \mu^{1/2}\rho,$$

where $\Delta\omega(\rho')$ takes a nonzero constant value only in the small region defining the pacemaker. Several shapes of the pacemaker were considered and the same qualitative results were obtained.

To perform numerical simulations of the partial differential equation (4), we divide the vessel into a network of $N \times N$ cells. In this network, the Laplacian operator ∇^2 , as well as the zero-flux boundary conditions, may be approximated by finite differences. It leads to a large system of coupled ordinary differential equations which can be integrated numerically by classical methods. We used a Runge-Kutta scheme, with a controlled time step.^{5,6} For most of the simulations in this paper the grid size was 80×80 . However, a system of 40×40 gave qualitatively the same results. On the other hand, a grid of 160×160 showed quantitatively equivalent results to the 80×80 system within an error of 10%.

Numerical simulations of Eq. (4) show that when $\Delta\omega = 0$, whatever the initial conditions, the asymptotic solution for Z is the homogeneous oscillation at frequency $\Omega_0 = -\beta$. However, when $\Delta\omega \neq 0$, target waves with

frequency $\Omega > \Omega_0$ are generated continuously under the influence of the pacemaker. These waves constitute a frequency-locked solution of Eq. (4) in compartment I. The relation between the frequency Ω of these concentric waves and the frequency shift $\Delta\omega$ of the pacemaker has been studied analytically by Hagan⁷ in the framework of the phase equation. Our simulations reported in Fig. 2 show that Ω is a highly nonlinear function of $\Delta\omega$, which exhibits a maximum for a given value of $\Delta\omega$, and decreases for $\Delta\omega > \Delta\omega_r$.

We also considered the case in which in compartment I two simultaneous pacemaker regions, with the same spatial extension and with different frequency shifts $\Delta\omega_1 < \Delta\omega_2$, were active. Target waves start to propagate from both centers, but after a while one sees that one of the centers remains active while the second one is prevented from emitting waves. The center which wins the competition is the one whose frequency Ω is the largest, as was predicted previously.^{7,8} It is interesting to note that although $\Delta\omega_1 < \Delta\omega_2$, because of the decreasing part of the function depicted in Fig. 2, target waves with a frequency $\Omega(\Delta\omega_1)$ can be seen in the system if $\Delta\omega_1$ is closer to $\Delta\omega_r$ than $\Delta\omega_2$.

Let us follow the events in compartment II. As a first simulation we consider a partition between the compartments with a single window size l taken as a control parameter. In this and in the three subsequent experiments, a single pacemaker region at point P is considered. When the first front starting from P in compartment I reaches the window, it generates a new set of similar target waves in compartment II. We want to know if the frequency of the waves in compartment II will lock onto the frequency Ω_I of the waves produced in compartment I. The simulations show that the frequency locking disappears when l is decreased below a critical value l_c .

Let us measure the phase difference $\phi_2 - \phi_1$ between the two oscillators of compartments II and I. For a window length of $l > l_c$, this phase difference tends to a stationary state ϕ ; therefore, in this case, frequency locking between the two compartments occurs [Fig. 1(a)]. However, as the size of the window l decreases, the stationary state ϕ tends to a limit point and the frequency-locked solution disappears at l_c [see Fig. 3(b)]. Below this value, a quasiperiodic solution is seen in the vicinity of the opening, and in compartment II, target waves propagate with a lower-frequency Ω_{II} compared to Ω_I in compartment I [Fig. 1(b)].

In order to understand better the behavior of the system in the vicinity of the opening and in the second compartment, for $l < l_c$, it is convenient to perform the change of variable $Z(\rho', \tau') = Y(\rho', \tau') \exp(i\Omega_I \tau')$. In terms of the variable Y , the frequency-locked solution which exists for $l > l_c$ appears as an inhomogeneous steady state $Y = Y_s$ of Eq. (4). However, for a smaller window, $l < l_c$, the steady state Y_s disappears in the

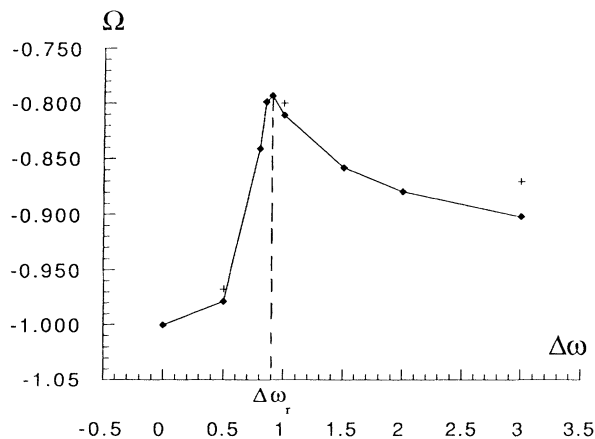


FIG. 2. Variation of the frequency Ω as a function of the local frequency shift $\Delta\omega$. Here the grid size is 40×40 , except for + corresponding to a grid of 80×80 . The other parameters are as in Fig. 1.

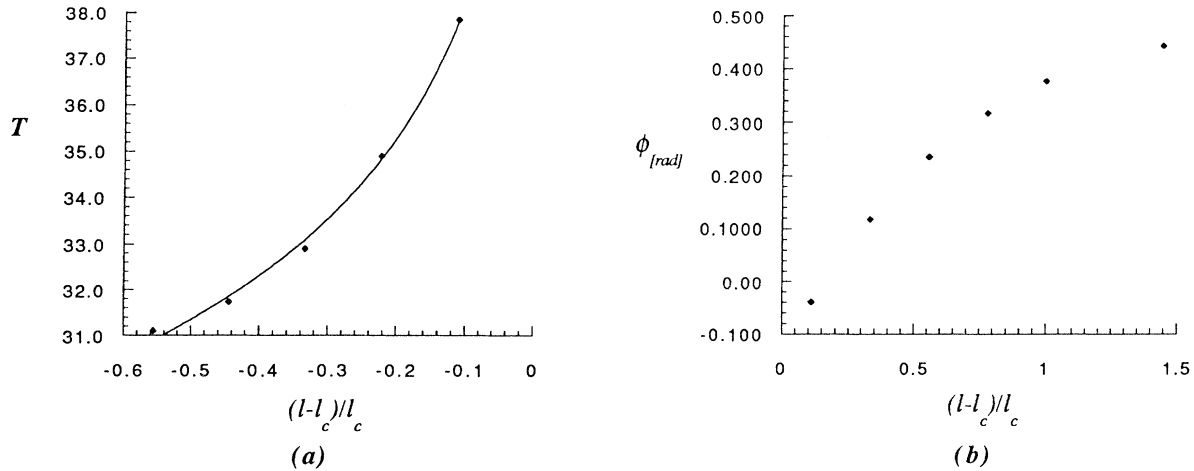


FIG. 3. (a) Period T of $Y(\rho', \tau')$ in compartment II as a function of the window size l . (b) Steady-state values of the phase difference ϕ as a function of l , for frequency-locked solutions. The parameters are the same as in Fig. 1.

second compartment and the dynamics of Y becomes periodic through an infinite-period bifurcation.

Figure 3(a) shows the relationship between the period T of the variable Y and the bifurcation parameter l . A curve fitting procedure on the numerical results indicates that this relationship is in good agreement with the law

$$l_c - l \propto \exp(-\lambda T) \tag{5}$$

which is the signature of a saddle-loop infinite-period bifurcation where a limit cycle merges with an unstable steady state.⁹

Therefore, in the vicinity of the window, the dynamics of Z becomes quasiperiodic when $l < l_c$, with independent frequencies Ω_I and $\gamma = 2\pi/T$. Moreover, in compartment II one observes that when the distance from the opening increases, Z follows periodic dynamics with only one frequency $\Omega_{II} = \Omega_I - \gamma$.

As l decreases, the wavelength of the target waves in compartment II increases. Thus if the size of the vessel is much smaller than the wavelength of the target waves, one sees only a weak concentration gradient which is only a fraction of the wavelength [Fig. 1(b)]. Therefore, in a finite system, target patterns are not observed in compartment II when the size l of the window becomes too small. This results from the fact that the wavelength is much larger than the size L of the system.

Let us now consider the same vessel and the same chemical reactions as described above. We introduce two openings l_1 and l_2 in the system [Figs. 4(a) and 4(b)]. Again a single local frequency shift $\Delta\omega$ is created at point P . Target waves with frequency Ω_I start to propagate in compartment I and reach successively the two openings l_1 and l_2 . For $\Delta\omega = 3$, the two windows act as new pacemaker regions and generate in turn target waves in the second compartment with $\Omega_{II}(l_1) = \Omega_{II}(l_2) = \Omega_I$. After a while, the target waves propagating from

the two centers collide and cusplike structures are formed [Fig. 4(a)].

In the next experiment, we only decrease $\Delta\omega$ at point P . A higher value of Ω_I , as compared with the preceding case, is obtained in the first compartment for the propagating target waves. In this experiment when the wave front reaches the windows l_1 and l_2 , new fronts are again generated. However, very soon the waves emerging from window l_2 take over the entire system and inhibit all propagation from l_1 [Fig. 4(b)].

A tentative explanation of this phenomenon is as follows. In this case one observes that $\Omega_{II}(l_1) < \Omega_{II}(l_2) \approx \Omega_I$. We saw in a preceding paragraph that if two pacemakers emit simultaneously, then the fastest waves inhibit the slower propagation and take over the entire system. As $\Omega_{II}(l_1) < \Omega_{II}(l_2)$ it is reasonable to think that a similar explanation prevails here. The frequency

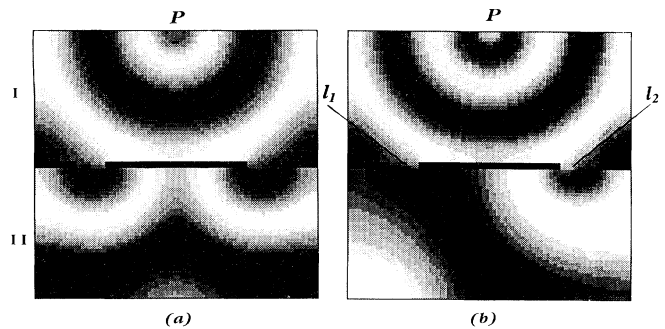


FIG. 4. Wave propagation in the presence of two windows. Parameters are as in Fig. 1, with $l_1 = 0.89l_c$, $l_2 = 1.1l_c$: (a) Waves propagate into compartment II from both windows and a cusplike structure is formed ($\Delta\omega = 3$). (b) Waves propagate from the largest window and inhibit the propagation from the small window ($\Delta\omega = 1$).

of the waves emerging from l_2 is fastest and therefore these waves take over the slowly evolving target waves which emerge from l_1 .

The simulation of other systems in the presence of walls and windows shows that, for some pacemaker positions, spiral waves may appear in compartment II.

The behavior found in our simulations must be contrasted to the property of sound waves or electromagnetic waves which in the experiment cited above would propagate from both apertures, producing interference effects. No such interference phenomena are seen with the target waves.

In a previous paper we discussed front propagation into a uniform state unstable with respect to a supercritical Hopf bifurcation.¹⁰ It was shown that due to the existence of a phase gradient, target waves were generated behind the front. According to the sign of β in the Ginzburg-Landau equation (4), the waves and the front travel in the same or in the opposite direction. In the latter case one sees incoming target waves traveling toward the pacemaker region. The incoming waves can also be seen in the oscillatory media depicted in Figs. 1 and 4.

Let us note that another peculiarity of unstable media is that, contrary to the oscillating systems described in this paper, there is no critical window length for target-wave propagation. As the medium is unstable, the smallest perturbation may trigger wave trains in part II.

The intriguing properties of dynamical systems described in this paper, in the case of continuous systems, may be also seen in networks of coupled oscillators. They can be used as analogical representations for solv-

ing specific problems encountered in artificial intelligence.¹¹

We are grateful to P. Gaspard, D. Keymeulen, and J. Decuyper for stimulating discussion. We are indebted to A. Destexhe for providing us with graphical software for spatiotemporal systems. J.A.S. is an Institut pour l'Encouragement de la Recherche Scientifique dans l'Industrie et l'Agriculture fellow.

¹G. Nicolis and I. Prigogine, *Self-Organization in Non-equilibrium Systems* (Wiley, New York, 1977).

²*Oscillations and Traveling Waves in Chemical Systems*, edited by R. J. Field and M. Burgers (Wiley, New York, 1985).

³Y. Kuramoto and T. Tzuzuki, *Prog. Theor. Phys.* **55**, 356 (1976).

⁴B. Bodet, J. Ross, and J. Vidal, *J. Chem. Phys.* **86**, 8 (1987).

⁵M. Kubicek and M. Marek, *Computational Methods in Bifurcation Theory and Dissipative Structures* (Springer-Verlag, New York, 1983).

⁶W. H. Press, B. P. Flannery, S. A. Teukolsky, and W. T. Vetterling, *Numerical Recipes. The Art of Scientific Computing* (Cambridge Univ. Press, Cambridge, 1986).

⁷P. S. Hagan, *Adv. Appl. Math.* **2**, 400 (1981).

⁸Y. Kuramoto and T. Yamada, *Prog. Theor. Phys.* **56**, 724 (1976).

⁹P. Gaspard, *J. Phys. Chem.* **94**, 1 (1990).

¹⁰J. A. Sepulchre, G. Dewel, and A. Babloyantz, *Phys. Lett. A* **147**, 380 (1990).

¹¹L. Steels, in *Proceedings of the European Conference in Artificial Intelligence 88*, edited by Y. Kadratoft (Pitman, London, 1989).

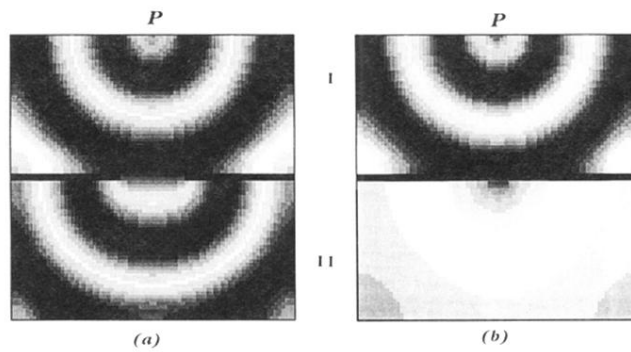


FIG. 1. (a),(b) A square vessel of side L is partitioned by a wall and communicates through a window of size l . A pacemaker region at P , where frequency is locally increased by $\Delta\omega$, generates target waves in compartment I, with a frequency Ω_1 . (a) The size of the window is $2l_c$ and in compartment II waves can propagate at the same frequency as in compartment I. (b) The size of the window is $\frac{2}{3}l_c$. No target waves are seen in compartment II for finite-size systems. The parameters of Eq. (4) are $\beta=1$, $\Delta\omega=1$. The critical window length is $l_c=5.03$ in units of the nondimensional space variable ρ' . The discretization of the vessel of side $L=44.8$ is 80×80 . The pacemaker at P is "T shaped," built on sixteen adjacent cells. The width of the wall is 1.12.

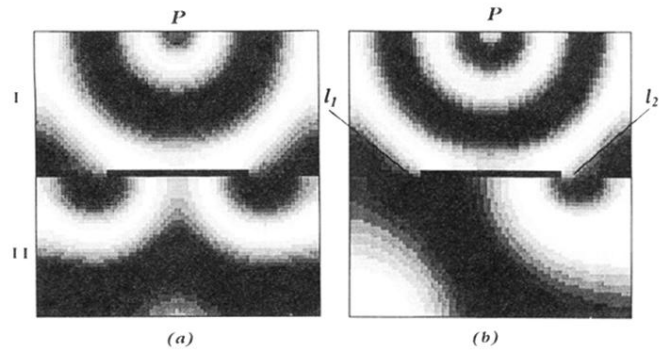


FIG. 4. Wave propagation in the presence of two windows. Parameters are as in Fig. 1, with $l_1=0.89l_c$, $l_2=1.1l_c$: (a) Waves propagate into compartment II from both windows and a cusplike structure is formed ($\Delta\omega=3$). (b) Waves propagate from the largest window and inhibit the propagation from the small window ($\Delta\omega=1$).